JACS
JOURNAL OF THE AMERICAN CHEMICAL SOCIETY

Communication

pubs.acs.org/JACS

Asymmetric Anion-π Catalysis: Enamine Addition to Nitroolefins on π-Acidic Surfaces

Yingjie Zhao,[†] Yoann Cotelle,[†] Alyssa-Jennifer Avestro,[†,‡] Naomi Sakai,[†] and Stefan Matile*[,†]

[†]Department of Organic Chemistry, University of Geneva, Geneva CH-1211, Switzerland

[‡]Department of Chemistry, Northwestern University, Evanston, Illinois 60208, United States

Supporting Information

ABSTRACT: Here we provide experimental evidence for anion-π catalysis of enamine chemistry and for asymmetric anion-π catalysis. A proline for enamine formation on one side and a glutamic acid for nitronate protonation on the other side are placed to make the enamine addition to nitroolefins occur on the aromatic surface of π-acidic naphthalenediimides. With increasing π acidity of the formally trifunctional catalysts, rate and enantioselectivity of the reaction increase. Mismatched and more flexible controls reveal that the importance of rigidified, precisely sculpted architectures increases with increasing π acidity as well. The absolute configuration of stereogenic sulfoxide acceptors at the edge of the π-acidic surface has a profound influence on asymmetric anion-π catalysis and, if perfectly matched, affords the highest enantio- and diastereoselectivity.

The stabilization of cationic transition states (TSs) and reactive intermediates on π-basic aromatic surfaces is common in biology[1,2] and increasingly appreciated in chemistry.[3,4] To demonstrate the stabilization of carbocation intermediates by cation-π interactions, i.e., the existence of cation-π catalysis, the increase of the stabilization of the cationic TS with increasing π basicity of the catalyst is considered convincing.[2,4] The same holds for increasing stereoselectivity with increasing π basicity as evidence for asymmetric cation-π catalysis.[4] Explicit experimental support that the charge-inverted anionic TSs can be stabilized on π-acidic surfaces has been reported only recently.[5−9] Initial support for the existence of anion-π catalysis has been secured with Kemp elimination.[5] Increasing stabilization of the anionic TS with increasing π acidity of the catalyst is evidence that anion-π interactions[9−12] can contribute to catalysis. To secure quantitative data on enolate intermediates, malonic acid diesters were positioned covalently on π-acidic surfaces.[6] Anion-π catalysis of enolate chemistry was elaborated with the selective addition of malonate half thioesters to enolate acceptors.[7]

Proline (Pro) catalysis adding aldehydes (**1**) to nitroolefins (**2** and **3**; Figure 1)[13] was selected to explore possible contributions of anion-π interactions to the stereochemistry of products **4** and **5**. This reaction was attractive because Wennemers et al. have demonstrated that the strategically positioned carboxylic acid in bifunctional catalyst **6** shifts the rate-limiting step from nitronate protonation in the original Jørgensen−Hayashi catalyst **7** to the formation of the C−C bond (Figure 1).[14] To build asymmetric anion-π catalysts, all that was needed was to insert a π-acidic surface between the Pro and the carboxylic acid in Wennemers **6**. Design, synthesis, and evaluation of these formally trifunctional catalysts are described below.

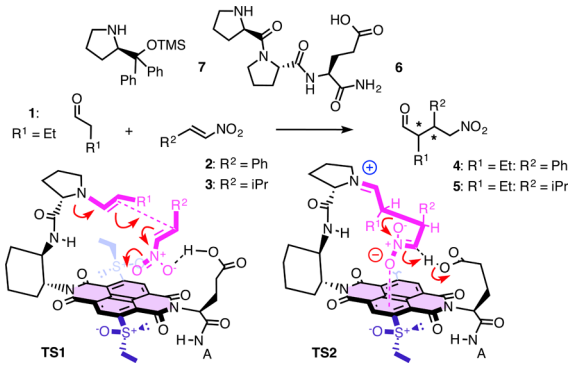

Figure 1. Structure of Wennemers and Jørgensen−Hayashi catalysts **6** and **7**, respectively, and possible stabilization of adding enamines (from aldehyde **1**) to nitroolefins **2** or **3** (**TS1**) and nitronate protonation (**TS2**) on the π-acidic surface of anion-π catalyst **9** (Figure 2).

Naphthalenediimides (NDIs)[15] were selected to construct asymmetric anion-π catalysts because their high intrinsic quadrupole moment was identified early on[12] as ideal to elaborate on anion-π interactions (in the range of TNT, more than twice that of hexafluorobenzene).[5] Two electron-donating sulfide substituents were installed in the NDI core of anion-π catalyst **8** (E_{LUMO} = −3.9 eV, Figure 2). Their gradual oxidation to electron-accepting sulfoxides as in **9** (E_{LUMO} = −4.4 eV) and sulfones as in **10** (E_{LUMO} = −4.6 eV) has evolved as a unique approach[16] to probe the importance of π acidity with minimal changes in global structure.[5,7,17−19] A Pro derivative was placed at one side of the π-acidic surface for enamine formation, a bit remote to leave space for the nitroolefin substrate to intercalate and keep the iminium intermediate away from the repulsive π-acidic surface. With an established Leonard turn,[5] the carboxylic acid was placed as close as possible at the other side of the NDI surface.

Initially, **1** should react with the Pro catalyst to yield the enamine, which is added to **2** or **3**.[14] With anion-π catalysts (e.g., **9**), the TS of this rate-limiting enamine addition could occur with parallel or perpendicular (**TS1**) orientation of the nitronate plane with respect to the π-acidic NDI surface (Figure 1). Both types of

Received: July 15, 2015
Published: September 8, 2015

DOI: 10.1021/jacs.5b07382
J. Am. Chem. Soc. 2015, 137, 11582−11585

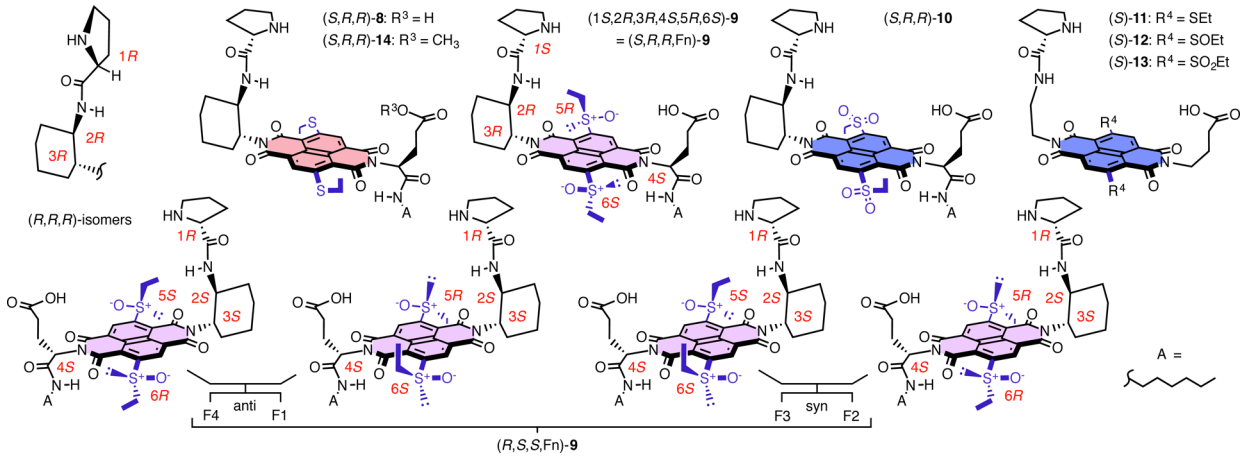

Figure 2. Structure of anion-π catalysts, with illustration of the mismatch with (*R*,*R*,*R*)-isomers and arbitrary numbering of the stereogenic centers. With 4*S* kept constant and centers 5 and 6 unknown beyond CD indications on syn or anti configuration (referred to as chiral HPLC fractions F1−F4), stereoisomers are designated on the basis of chiral centers 1−3 as shown.

nitrate-π interactions have been observed, even in the same crystal.[11] According to molecular models, orthogonal orientation of the nitronate appears preferable to produce syn products (**TS1**) and is necessary for intramolecular protonation of the nitronate (**TS2**). Carboxylate-π interactions[5] in the resulting reactive intermediate will ensure the removal of the product from the aromatic surface.

Synthesis of the complete set of stereoisomers of anion-π catalyst **8** was very straightforward (Figure 2; Schemes S1−S3). Anion-π catalyst (*S*)-**11** was added to the collection as a more flexible, adaptive system with only one stereogenic center of the Pro. Sulfide oxidation with mCPBA at low temperature gave more rigid **9** and more flexible **12** with two sulfoxides on the core, but oxidation at room temperature gave anion-π catalysts **10** and **13** with two sulfones. Co-injection of Boc-protected (*S*,*R*,*R*)-**8** and (*R*,*R*,*R*)-**8** in chiral HPLC gave baseline-separated peaks; the individual samples gave only one peak each without traces from the other (Figure S6). This demonstrates the enantiopurity of the catalysts and the absence of permanent additional axial chirality.

Reaction kinetics were measured with 1.0 M **1**, 500 mM **2** or **3**, and 50 mM **8**−**14** in $CDCl_3/CD_3OD$ 1:1 at room temperature. Reactions were followed directly by ^1H NMR spectroscopy (Figures S3 and S4). Product mixtures were analyzed by chiral HPLC (Figure S7; Table 1). The observed syn diastereoselectivity and enantioselectivities were consistent with those of other Pro-based catalysts.[13,14] Initial controls confirmed that reactions went to completion within 24 h and total yields were nearly quantitative (Figures S3 and S4). Control catalyst **14** with a methyl ester in place of the carboxylic acid was nearly inactive (Figure S5). This result was important because it confirmed[14] not only that the presence of the carboxylic acids is essential but also that the reaction takes place between the Pro and the glutamic acid on the π-acidic surface.

The rate of the reaction increased from least π-acidic catalysts **8** to most π-acidic catalysts **10**. Observed rate enhancements calculated to a decrease in activation energy of ΔE_a = −2.8 to −3.9 kJ mol^{-1} (Table 1, entries 1−5 and 26−29; Figure 3A, blue rectangles). Decreasing activation energies with increasing π acidity were almost independent of the chirality of catalysts **10**; only the more flexible control **13** was clearly less responsive to changes in π acidity, i.e., anion-π catalysis (Figure 3A, blue X). Similar rate enhancements observed for **5** indicated that the phenyl group in **2** is not decisive (Figure 1).

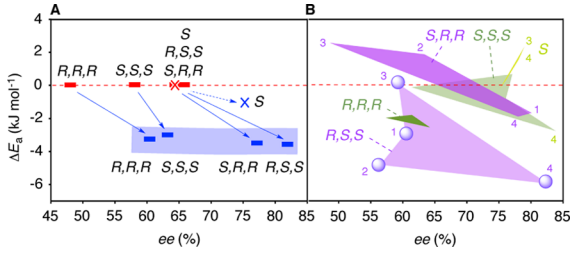

Figure 3. Kinetic chiral space covered by catalysts (A) **8**, **10**, and (B) **9**. (A) ΔE_a for the reaction of **1** with **2** in the presence of **10** (blue rectangles; **13**, blue X) compared to **8** (red rectangles; **11**, red X), and ee of **4** obtained with **8** (red rectangles), **10** (blue rectangles), **11** (red X), and **13** (blue X). Blue arrows: Change with increasing π acidity. (B) ΔE_a for the reaction of **1** with **2** in the presence of **9** compared to **8** (dotted red line) and ee of **4** obtained with **9**, reported as the area covered by the four sulfoxide stereoisomers F1−F4 of each stereoisomer of **9**. Shaded circles: F1−F4 of (*R*,*S*,*S*)-**9**.

Decreasing activation energies with increasing π acidity of the catalyst resulted in higher enantioselectivity. The enantiomeric excess (ee) with **4** obtained with the most π-acidic catalysts **10** (blue rectangles) or **13** (blue X) always exceeded that with least π-acidic catalysts **8** (red rectangles) or **11** (red X) independent of number and configuration of stereogenic centers in the catalysts (Figure 3A). Considering the understood importance of higher selectivity at faster rates in bifunctional catalysis,[20] this general increase of both with increasing π acidity in nearly isostructural catalysts supported the idea that anion-π interactions generally contribute to enantioselectivity, i.e., the existence of asymmetric anion-π catalysis.

Consideration of the full chiral product space[21] revealed that at minimal π acidity ee and the diastereomeric ratio dr of the four diastereomers of catalyst **8** scatter broadly with less convincing stereoselectivities (Figure 4A, red squares). At maximal π acidity, the four diastereomers of catalyst **10** line up nicely and separate into matched and mismatched architectures (Figure 4A, blue circles). (*R*,*S*,*S*)-Diastereomer **10** emerged as the best catalyst, closely followed by (*S*,*R*,*R*)-**10** (Table 1, entries 26 and 29). Molecular models confirmed that in the mismatched (*R*,*R*,*R*)- and (*S*,*S*,*S*)-isomers the pyrrolidine ring is turned away and has to be forced into a more strained conformation to position the reaction on the π-acidic surface and to reach the essential carboxylic acid on the other side (Figures 1 and 2). More flexible

DOI: 10.1021/jacs.5b07382
J. Am. Chem. Soc. 2015, 137, 11582−11585

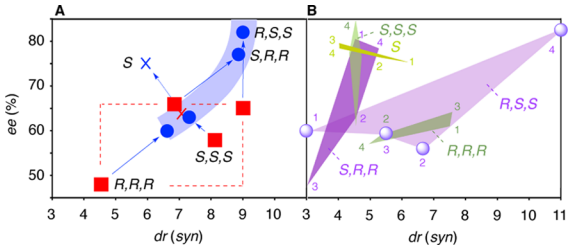

Figure 4. Full chiral space covered by (A) **8**, **10**, and (B) **9**. (A) dr and ee for **4** obtained with **8** (red squares), **10** (blue circles), **11** (red X) and **13** (blue X). Blue arrows connect identical stereoisomers at minimal (red symbols) and maximal π acidity (blue symbols). (B) Chiral space with ee and dr for **4** obtained with **9**, reported as the area covered by the four sulfoxide stereoisomers F1–F4 of each stereoisomer. Shaded circles: F1–F4 of (*R*,*S*,*S*)-**9**.

Table 1. Characteristics of Anion-π Catalysts.[a]

	cat[b]	configuration[c]	ΔE_a (kJ/mol)[d]	dr[e]	ee (%)[f]
1	**8**	1*S*,2*R*,3*R*	0	6.9:1	66
2	**8**	1*R*,2*R*,3*R*	0	4.5:1	−48
3	**8**	1*S*,2*S*,3*S*	0	8.1:1	58
4	**8**	1*R*,2*S*,3*S*	0	9.0:1	−65
5	**11**	1*S*	0	7.0:1	64
6	**9**	1*S*,2*R*,3*R*,F1 (anti)	−1.7	4.5:1	80
7	**9**	1*S*,2*R*,3*R*,F2 (syn)	+1.9	4.5:1	63
8	**9**	1*S*,2*R*,3*R*,F3 (anti)	+2.6	3.0:1	48
9	**9**	1*S*,2*R*,3*R*,F4 (syn)	−1.9	5.2:1	78
10	**9**	1*R*,2*R*,3*R*,F1 (anti)	−1.8	7.4:1	−61
11	**9**	1*R*,2*R*,3*R*,F2 (syn)	−1.9	5.3:1	−59
12	**9**	1*R*,2*R*,3*R*,F3 (syn)	−2.6	7.5:1	−64
13	**9**	1*R*,2*R*,3*R*,F4 (anti)	−2.0	4.9:1	−57
14	**9**	1*S*,2*S*,3*S*,F1 (anti)	+0.7	4.3:1	77
15	**9**	1*S*,2*S*,3*S*,F2 (syn)	−0.8	4.7:1	76
16	**9**	1*S*,2*S*,3*S*,F3 (syn)	−0.1	4.5:1	61
17	**9**	1*S*,2*S*,3*S*,F4 (anti)	−2.8	4.5:1	83
18	**9**	1*R*,2*S*,3*S*,F1 (anti)	−3.0	3.1:1	−60
19	**9**	1*R*,2*S*,3*S*,F2 (syn)	−4.9	6.7:1	−56
20	**9**	1*R*,2*S*,3*S*,F3 (syn)	+0.1	5.3:1	−59
21	**9**	1*R*,2*S*,3*S*,F4 (anti)	−5.9	10.9:1	−82
22	**12**	1*S*,F1 (syn)	−0.2	6.1:1	75
23	**12**	1*S*,F2 (anti)	+0.3	5.3:1	76
24	**12**	1*S*,F3 (syn)	+2.4	4.0:1	79
25	**12**	1*S*,F4 (anti)	+1.6	4.0:1	78
26	**10**	1*S*,2*R*,3*R*	−3.4	8.9:1	77
27	**10**	1*R*,2*R*,3*R*	−3.1	6.6:1	−60
28	**10**	1*S*,2*S*,3*S*	−2.8	7.3:1	63
29	**10**	1*R*,2*S*,3*S*	−3.9	9.0:1	−82
30	**13**	1*S*	−1.1	5.9:1	76

[a]Measured with 1.0 M **1**, 500 mM **2**, and 50 mM catalyst in $CDCl_3$/CD_3OD 1:1, at room temperature. [b]Catalysts; see Figure 2. [c]Arbitrary numbering; see Figure 2. [d]Rate enhancement, negative = acceleration, positive = deceleration, $\Delta E_a = -RT \ln(v_{ini}/v_{ini}^0)$; v_{ini}^0 = initial velocity with **8** or **11**. [e]Diastereomeric ratio, for syn isomer. [f]Enantiomeric excess, a negative ee indicates preference for the opposite enantiomer of the product.

control **13** at maximal π acidity performed comparably well with regard to ee but, as with poor rate enhancements (Figure 3A, blue X), failed to yield high diastereoselectivity (Figure 4A, blue X; Table 1, entry 30). This demonstrates that contrary to the uniform increase of enantioselectivity with π acidity (Figure 3A, blue arrows) diastereoselectivity depends also on precisely sculpted architectures around the π-acidic surface (Figure 4A, blue arrows).

At intermediate π acidity, **9** and **12** were special because two additional chiral centers are introduced right at the edge of the π surface. All four diastereomers of **9** and **12** could be separated by chiral HPLC (Figure S1). In their circular dichroism (CD) spectra,[22] 2 of the 4 fractions collected by HPLC always showed strong and nearly mirror-imaged Cotton effects at long wavelength (Figure S2). Comparison with previously reported CD spectra and crystal structures[18,19] suggested that these contain the syn isomers (Figure 2). In syn isomers, the preferred in-plane orientation of the conjugated S-O turns both ethyl groups to the same side of the aromatic plane.

The reaction of **1** with **2** in the presence of **9** was conducted under the conditions introduced above. Contrary to the consistent increases in rate and enantioselectivity from less π-acidic **8** to more π-acidic **10** (Figure 3A), stereoselective transition-state stabilization by chiral sulfoxides at the edge of the π-acidic surface of **9** was more complex. Judged from the area covered in the kinetic chiral space, mismatched and more flexible catalysts were not very sensitive to the chirality of the sulfoxides at the π surface (Figure 3B, olive). Best in this series was (*S*,*S*,*S*,F4)-**9** (Table 1, entry 17), but other catalysts suffered from poor rate enhancement ((*S*,Fn)-**9**, Table 1, entries 22–25), poor enantioselectivity ((*R*,*R*,*R*)-**9**, Table 1, entries 10–13), or both.

The kinetic chiral space covered by the matched catalysts was most impressive (Figure 3B, magenta). Dependent only on the chirality of the sulfoxides at the edge of the π surface of (*S*,*R*,*R*)-**9**, strong deceleration with poor enantioselectivity (F3) could change to strong acceleration with good enantioselectivity (F1 and F4, Figure 3B; Table 1, entries 6–9). (*R*,*S*,*S*)-**9** showed poor enantioselectivity at broadly varied rates except for the outstanding (*R*,*S*,*S*,F4)-**9** (Figure 3B and Table 1, entries 18–21). The ΔE_a = −5.9 kJ mol^{-1} of (*R*,*S*,*S*,F4)-**9** is the most significant rate enhancement found in the entire series. It exceeded by far the similarly enantioselective ΔE_a = −3.9 kJ mol^{-1} of the more π-acidic (*R*,*S*,*S*)-**10**.

The full chiral space covered by the variation of the chirality of the sulfoxides at the edge of the π surface was similarly impressive (Figure 4B and Table 1, entries 6–25). Highest sensitivity was again found for matched catalysts (*S*,*R*,*R*)-**9** and particularly (*R*,*S*,*S*)-**9** (Figure 4B, magenta), but mismatched and flexible catalysts covered much less chiral space (Figure 4B, olive). Good enantioselectivity was observed with some isomers containing *S*-Pro, i.e., (*S*,*R*,*R*)-**9**, (*S*,*S*,*S*)-**9**, and (*S*)-**9**, but good diastereoselectivity occurred with selected isomers containing *R*-Pro, i.e., (*R*,*R*,*R*)-**9** and (*R*,*S*,*S*)-**9**. Only one catalyst, (*R*,*S*,*S*,F4)-**9**, showed good enantioselectivity and diastereoselectivity (Figure 4B and Table 1, entry 21). This hypersensitivity to topological matching suggested that the absolute configuration at the glutamate side kept constant in *S* throughout the study is also essential; otherwise (*S*,*R*,*R*)-**9** would be as good as (*R*,*S*,*S*)-**9**. As for rate enhancements, diastereoselectivity of (*R*,*S*,*S*,F4)-**9** exceeded significantly even that of the more π-acidic (*R*,*S*,*S*)-**10** (Figure 4A,B). CD spectrum suggested that the stereochemistry of (*R*,*S*,*S*,F4)-**9** (the best catalyst found in this study) is anti (Figure S2); discrimination between the (5*S*,6*R*)- and (5*R*,6*S*)-diastereomers requires information from crystal structures (Figure 2).

Our results provide unprecedented experimental support that anion-π interactions[9] can contribute to asymmetric enamine catalysis. Generally increasing enantioselectivity and rates with increasing π acidity of nearly isostructural catalysts are

DOI: 10.1021/jacs.5b07382
J. Am. Chem. Soc. 2015, 137, 11582–11585

particularly important[20] with regard to existence and relevance of asymmetric anion-π catalysis (Figure 3A). The relationship between diastereoselectivity and π acidity of stereoisomeric catalysts is more complex (Figure 4A) and, like the profound impact of chiral centers right at the edge of their π-acidic surface (Figures 3B and 4B), nicely highlights the importance of rigidified and "matched" architectures around the central π-acidic surface. Current efforts focus on larger substituents for the chiral sulfoxides at the edge of the π-acidic surface[19] to reach more significant stereoselectivities, on determination of their absolute configuration in refined catalysts,[18,19] and on anion-π catalysts for otherwise difficult reactions[13c] and their integration into more complex systems.[23]

■ ASSOCIATED CONTENT

Supporting Information

The Supporting Information is available free of charge on the ACS Publications website at DOI: 10.1021/jacs.5b07382.

Detailed experimental procedures. (PDF)

■ AUTHOR INFORMATION

Corresponding Author

*stefan.matile@unige.ch

Present Address

Y.Z.: Institute of Polymers, ETH Zurich, Zurich 8093, Switzerland, and Qingdao University of Science and Technology, Qingdao, Shandong 266042, China.

Notes

The authors declare no competing financial interest.

■ ACKNOWLEDGMENTS

We thank the NMR and Sciences Mass Spectrometry platforms for services, and the University of Geneva, the European Research Council (ERC Advanced Investigator), the Swiss National Centre of Competence in Research Chemical Biology, the NCCR Molecular Systems Engineering and the Swiss NSF for financial support. A.-J.A. thanks the US National Science Foundation for the award of a Graduate Research Opportunities Worldwide Fellowship (grant no. SP0027231; Project 60037460) and the Swiss State Secretariat for Education Research and Innovation and Federal Commission for Scholarships for the award of a Government Excellence Scholarship for Foreign Students in support of this research.

■ REFERENCES

(1) Dougherty, D. A. *Acc. Chem. Res.* **2013**, *46*, 885−893.

(2) Faraldos, J. A.; Antonczak, A. K.; Gonzalez, V.; Fullerton, R.; Tippmann, E. M.; Allemann, R. K. *J. Am. Chem. Soc.* **2011**, *133*, 13906−13909.

(3) (a) Yamada, S.; Fossey, J. S. *Org. Biomol. Chem.* **2011**, *9*, 7275−7281. (b) Zhang, Q.; Tiefenbacher, K. *Nat. Chem.* **2015**, *7*, 197−202.

(4) (a) Knowles, R. R.; Lin, S.; Jacobsen, E. N. *J. Am. Chem. Soc.* **2010**, *132*, 5030−5032. (b) Holland, M. C.; Metternich, J. B.; Mück-Lichtenfeld, C.; Gilmour, R. *Chem. Commun.* **2015**, *51*, 5322−5325.

(5) (a) Zhao, Y.; Domoto, Y.; Orentas, E.; Beuchat, C.; Emery, D.; Mareda, J.; Sakai, N.; Matile, S. *Angew. Chem., Int. Ed.* **2013**, *52*, 9940−9943. (b) Zhao, Y.; Beuchat, C.; Mareda, J.; Domoto, Y.; Gajewy, J.; Wilson, A.; Sakai, N.; Matile, S. *J. Am. Chem. Soc.* **2014**, *136*, 2101−2111.

(6) Zhao, Y.; Sakai, N.; Matile, S. *Nat. Commun.* **2014**, *5*, 3911.

(7) Zhao, Y.; Benz, S.; Sakai, N.; Matile, S. *Chem. Sci.* **2015**, DOI: 10.1039/C5SC02563J.

(8) Berkessel, A.; Das, S.; Pekel, D.; Neudörfl, J. M. *Angew. Chem., Int. Ed.* **2014**, *53*, 11660−11664.

(9) In analogy to cation-π interactions, "anion-π interactions" is used in here to refer to the site of the interaction (i.e., on the aromatic π surface, orthogonal to the plane with distances around or preferably shorter than the sum of the VdW radii) without any implications on the nature of the interaction (Q_{zz} quadrupoles, in-plane multipoles, etc.).[10−12] Complementary to cation-π interactions, anion-π interactions relate to LUMO chemistry; "too strong" anion-π interactions lead to charge-transfer complexes and radicals (comparable to proton transfer and conjugate acids and bases with "too strong" H bonds) and to nucleophilic aromatic substitution.

(10) (a) Frontera, A.; Gamez, P.; Mascal, M.; Mooibroek, T. J.; Reedijk, J. *Angew. Chem., Int. Ed.* **2011**, *50*, 9564−9583. (b) Chifotides, H. T.; Dunbar, K. R. *Acc. Chem. Res.* **2013**, *46*, 894−906. (c) Salonen, L. M.; Ellermann, M.; Diederich, F. *Angew. Chem., Int. Ed.* **2011**, *50*, 4808−4842. (d) Kumar, S.; Ajayakumar, M. R.; Hundal, G.; Mukhopadhyay, P. *J. Am. Chem. Soc.* **2014**, *136*, 12004−12010. (e) Fujisawa, K.; Humbert-Droz, M.; Letrun, R.; Vauthey, E.; Wesolowski, T. A.; Sakai, N.; Matile, S. *J. Am. Chem. Soc.* **2015**, *137*, 11047−11056. (f) Schneebeli, S. T.; Frasconi, M.; Liu, Z.; Wu, Y.; Gardner, D. M.; Strutt, N. L.; Cheng, C.; Carmieli, R.; Wasielewski, M. R.; Stoddart, J. F. *Angew. Chem., Int. Ed.* **2013**, *52*, 13100−13104.

(11) (a) Adriaenssens, L.; Estarellas, C.; Vargas Jentzsch, A.; Martinez Belmonte, M.; Matile, S.; Ballester, P. *J. Am. Chem. Soc.* **2013**, *135*, 8324−8330. (b) Giese, M.; Albrecht, M.; Ivanova, G.; Valkonen, A.; Rissanen, K. *Supramol. Chem.* **2012**, *24*, 48−55. (c) Wang, D.-X.; Wang, M.-X. *J. Am. Chem. Soc.* **2013**, *135*, 892−897. (d) Watt, M. M.; Zakharov, L. N.; Haley, M. M.; Johnson, D. W. *Angew. Chem., Int. Ed.* **2013**, *52*, 10275−10280. (e) Vargas Jentzsch, A.; Hennig, A.; Mareda, J.; Matile, S. *Acc. Chem. Res.* **2013**, *46*, 2791−2800.

(12) Gorteau, V.; Bollot, G.; Mareda, J.; Perez-Velasco, A.; Matile, S. *J. Am. Chem. Soc.* **2006**, *128*, 14788−14789.

(13) (a) Marigo, M.; Wabnitz, T. C.; Fielenbach, D.; Jørgensen, K. A. *Angew. Chem., Int. Ed.* **2005**, *44*, 794−797. (b) Hayashi, Y.; Gotoh, H.; Hayashi, T.; Shoji, M. *Angew. Chem., Int. Ed.* **2005**, *44*, 4212−4215. (c) Jensen, K. L.; Dickmeiss, G.; Jiang, H.; Albrecht, L.; Jørgensen, K. A. *Acc. Chem. Res.* **2012**, *45*, 248−264. (d) Seebach, D.; Sun, X.; Sparr, C.; Ebert, M.-O.; Schweizer, W. B.; Beck, A. K. *Helv. Chim. Acta* **2012**, *95*, 1064−1078. (e) Uehara, H.; Barbas, C. G., III *Angew. Chem., Int. Ed.* **2009**, *48*, 9848−9852.

(14) (a) Duschmale, J.; Wiest, J.; Wiesner, M.; Wennemers, H. *Chem. Sci.* **2013**, *4*, 1312−1318. (b) Wiesner, M.; Revell, J. D.; Wennemers, H. *Angew. Chem., Int. Ed.* **2008**, *47*, 1871−1874.

(15) (a) Bhosale, S. V.; Jani, C. H.; Langford, S. J. *Chem. Soc. Rev.* **2008**, *37*, 331−342. (b) Suraru, S. L.; Würthner, F. *Angew. Chem., Int. Ed.* **2014**, *53*, 7428−7448. (c) Das, A.; Ghosh, S. *Angew. Chem., Int. Ed.* **2014**, *53*, 2038−2054. (d) Chong, Y. S.; Dial, B. E.; Burns, W. G.; Shimizu, K. D. *Chem. Commun.* **2012**, *48*, 1296−1298. (e) Ponnuswamy, N.; Pantoş, G. D.; Smulders, M. M. J.; Sanders, J. M. K. *J. Am. Chem. Soc.* **2012**, *134*, 566−573. (f) Gabriel, G. J.; Iverson, B. L. *J. Am. Chem. Soc.* **2002**, *124*, 15174−15175.

(16) (a) Dado, G. P.; Gellman, S. H. *J. Am. Chem. Soc.* **1993**, *115*, 12609−12610. (b) Kramer, J. R.; Deming, T. J. *J. Am. Chem. Soc.* **2014**, *136*, 5547−5550.

(17) Misek, J.; Vargas Jentzsch, A.; Sakurai, S.; Emery, D.; Mareda, J.; Matile, S. *Angew. Chem., Int. Ed.* **2010**, *49*, 7680−7683.

(18) Lin, N.-T.; Vargas Jentzsch, A.; Guénée, L.; Neudörfl, J.-M.; Aziz, S.; Berkessel, A.; Orentas, E.; Sakai, N.; Matile, S. *Chem. Sci.* **2012**, *3*, 1121−1127.

(19) Zhao, Y.; Huang, G.; Besnard, C.; Mareda, J.; Sakai, N.; Matile, S. *Chem. - Eur. J.* **2015**, *21*, 6202−6207.

(20) Copeland, T. G.; Miller, S. J. *J. Am. Chem. Soc.* **2001**, *123*, 6496−6502.

(21) Lichtor, P. A.; Miller, S. J. *J. Am. Chem. Soc.* **2014**, *136*, 5301−5308.

(22) Donnoli, M. I.; Giorgio, E.; Superchi, S.; Rosini, C. *Org. Biomol. Chem.* **2003**, *1*, 3444−3449.

(23) (a) Baumeister, B.; Sakai, N.; Matile, S. *Org. Lett.* **2001**, *3*, 4229−4232. (b) Sakai, N.; Sordé, N.; Matile, S. *J. Am. Chem. Soc.* **2003**, *125*, 7776−7777.